

# Electrochemical evaluation of quinolin-8-ol derivatives for carbon steel protection

A.A. El-Bindary<sup>1,\*</sup>, K.S. El-Alfy<sup>2</sup>, M.H. Mahmoud<sup>3</sup>, O.M. Diwan<sup>3</sup>

<sup>1</sup>Chemistry Department, Faculty of Science, Damietta University, Damietta 34517, Egypt

<sup>2</sup>Irrigation Engineering and Hydraulics Department, Faculty of Engineering, Mansoura University, Mansoura, Egypt

<sup>3</sup>Department of Mathematical and Physical Engineering, Faculty of Engineering, Mansoura University, Mansoura, Egypt

\*Corresponding author: E-mail address: [abindary@yahoo.com](mailto:abindary@yahoo.com) (A.A. El-Bindary)

**Abstract:** The inhibitive effect of new eco-friendly quinolin-8-ol derivatives against C-steel and its adsorption behavior were investigated in 2 M HCl solution utilized mass reduction, tafel polarization, (EIS) electrochemical impedance spectroscopy and (EFM) electrochemical frequency modulation method. The data obtain from protective efficiency rise with the improving the dose of inhibitor. The orders of %IE of quinolin-8-ol derivatives are given: (1) > (2) > (3). The temperature effect on corrosion protection has been worked and the thermodynamic activation and adsorption parameters were measured. It seems that the lower in corrosion protection efficiency with improving temperature led to desorption of adsorbed inhibitor molecules occur. The type of quinolin-8-ol derivatives are mixed inhibitor whose adsorption habit onto C-steel can be well found by isotherm Freundlich equation. EIS spectra exhibit one capacitive loop and confirm the protective ability.

**Keywords:** Quinolin-8-ol, Adsorption, C-steel, SEM-EDX.

## 1. Introduction

Corrosive arrangements are mainly utilized as a part of industry, for example, corrosive pickling of steel and iron, substance cleaning and preparing, generation of metal and well oil fermentation [1–3]. The issues increase from acid corrosion needed the improvement of different corrosion control methods among which the application of chemical inhibitors has been information as most economical tests for preclude corrosion of acid [4–9]. Numerous organic compounds, such as heterocyclic compounds, quaternary ammonium salts and acetylenic alcohol are generally utilized as inhibitors in different industries. The normal atoms adsorb on the metal surface among hetero atom, such as sulfur nitrogen and oxygen prevent the active sites and lead to a physical barrier to lower the transport of erosion species to the surface of metal [10–16]. Different inquires about uncovered that the influenced of adsorption not only the charge surface and nature of the metal, but also by the chemical assembled of inhibitors. The heterocyclic substances include N atoms, such as 4-aminoantipyrine are good corrosion protective with corrosive solution due to rise inhibition protection, best thermal stability and prevent the odor irritating for alloys and metals in different aggressive solution [17–22]. Therefore, the improve of novel adjuster inhibitors include 4-aminoantipyrineheterocyclic ring and the research of the relations among the chemicalstructure of inhibitors and their protection led to the higher significance in theoretical points and industrial.

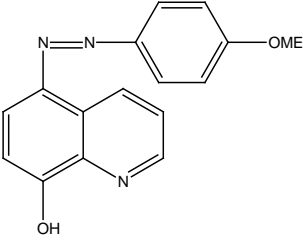
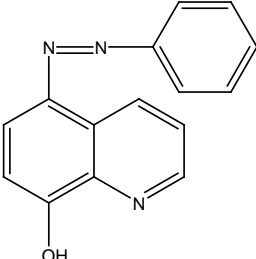
In this study, the protection effect and electrochemical habit of quinolin-8-ol derivatives for C-steel contain 2 molar hydrochloric acid are given by the mass reduction method, tafel polarization, (EIS) and (EFM) tests. A few quantum-chemistry measurements have been obtain in order to record the inhibition protection to the molecular properties of the various kind of compounds [23,24]. SEM and EDX examination of the C-steel in 2 M HCl surface revealed that these compounds prevented C-steel in 2 M HCl from corrosion by adsorption on its surface to form a protective film and acts as a barrier to corrosive media.

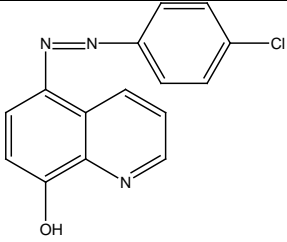
## 2. Experimental

### 2.1. Material and medium

Carbon steel was utilized for the calculation of corrosion. It's percent composition is 0.20 C, 0.30 Si, 0.53 Mn, 0.055 S, 0.045 P, the rest iron. The corrosion dose (2 M HCl) (37% analytical grade,) was ready by hydrochloric acid dilution with water double distilled. Quinolin-8-ol derivatives utilized for this paper, whose structures were given in Table 1 [25-27]. 25 ml of water distilled with 0.01 M hydrochloric acid are appending to aniline (0.01 mol) or its p-derivatives. A dose of 0.01 M NaNO<sub>3</sub> in 20 ml of water is putted drop wise to the mixture obtained then stirred and cooled to 0 °C. The structure of diazonium chloride is coupled consecutively attendance an alkaline dose of 0.01 M quinolin-8-ol, in 10 ml of pyridine.

**Table 1:** Molecular formulas and structure of quinolin-8-ol derivatives.

Compound	Structure	Empirical formula	Molecular weight
(1)	 <p>5-(2-(4-Methoxyphenyl)diazenyl)quinolin-8-ol</p>	C <sub>16</sub> H <sub>13</sub> N <sub>3</sub> O <sub>2</sub>	279
(2)	 <p>5-(2-Phenyldiazenyl)quinolin-8-ol</p>	C <sub>15</sub> H <sub>11</sub> N <sub>3</sub> O	249

<b>(3)</b>	 <p>5-(2-(4-Chlorophenyl)diazenyl)quinolin-8-ol</p>	$C_{15}H_{10}N_3OCl$	283.5
------------	--	----------------------	-------

## 2.2. Methods

### 2.2.1. Mass reduction method

Coins of CS with dimensions 20 x 20 x 2 ml were abraded with various emery papers. After accurately weighting, the coins were putted in 100 ml of two molar hydrochloric acid lack attendance various dose of inhibitors at  $(30 \pm 1^\circ C)$ . After various periods immersion, the steel tests were washed by bi-distilled water then dried and weighted second. The mass reduction data are utilized to measured the rate of corrosion (R) in  $mm\text{y}^{-1}$  by Eq. (1):

$$R = (8.75 \times 10^4 \times \text{mass loss in gram}) / \text{DAT} \quad (1)$$

T = time exposure in hr, D = density of iron in  $g\text{ cm}^{-3}$ , A = area covered in  $\text{cm}^2$ . The protection efficiency (%IE) and the ( $\theta$ ) were measured from Eq. (2):

$$\%IE = 100 \times \theta = 100 \times [(R^* - R) / R^*] \quad (2)$$

$R^*$  = the rates of corrosion of CS in the lack of inhibitor and R = the rates of corrosion of CS with inhibitor.

### 2.2.2. Electrochemical tests

Electrochemical tests were lead to three electrodes cell thermostatic utilized a Gamrypotentiostat/galvanostat/ZRA (model PCI300/4). A saturated calomel and platinum electrode were utilized as reference and auxiliary electrodes. The CS electrodes were 10x10 ml and were welded with a copper wire on one side. All method were done at temperature  $(30 \pm 1^\circ C)$ . The potentiodynamic diagrams were measured from -50 to 50 V at a rate scan  $1\text{ mV S}^{-1}$  after the steady state is approached (30 min) and the open potential circuit was observed after putted the electrode for 15 min in the solution test. The ( $\theta$ ) and % IE were measured from Eq. (3):

$$\%IE = 100\theta \times = 100 \times [1 - (i^{\circ}_{\text{corr}} / i_{\text{corr}})] \quad (3)$$

$i^{\circ}_{\text{corr}}$  and  $i_{\text{corr}}$  are the current corrosion densities lack and attendance of solution inhibitor, consecutively.

(EFM) and (EIS) tests were obtain by utilized the same methods as before with a Gamry framework system depend on ESA400. Echem Analyst 5.5 Software was utilized for drawing, graphing and fitting

data. EIS tests were done in a range of frequency of 100 kHz to 10 mHz with amplitude of 5 mV peak-to-peak ac signals utilized at respective for potential corrosion. EFM had done utilized 2 frequencies 2 and 5 Hz. The frequency base was 1 Hz. In this research, we utilized a signal perturbation with amplitude of 10 mV for both frequencies perturbation of 2 and 5 Hz.

### 2.2.3. SEM-EDX tests

The surface of CS was obtain by keeping the coins for 3 days putted in 2 M hydrochloric acid with and lack of perfect dose of quinolin-8-ol derivatives, after abraded mechanically utilized unlike papers emery up to grit size 1200. Then, after this time immersion, the samples were lotion gently with distilled water, carefully dried and mounted into the spectrometer attendance of further treatment. The surface of alloy were tested utilized an X-ray diffractometer Philips (pw-1390) with Cu-tube ( $\text{CuK}\alpha$ ,  $\lambda = 1.54051 \text{ \AA}$ ), (SEM, JOEL, JSM-T20, Japan).

## 3. Results and discussion

### 3.1. Mass reduction tests

The time -mass reduction diagrams for the corrosion of alloy in 2 M acid without and with unlike dose of Compound (1) at  $30 \pm 1^\circ\text{C}$  given in Fig. 1. The same plots for other compounds were given and are not show. The data of Table 2 given that, the (%IE) improve with rise in dose of inhibitor from  $1 \times 10^{-6}$  to  $11 \times 10^{-6}$  M. The higher (%IE) was obtaining at  $11 \times 10^{-6}$  M. The protection efficiency (%IE) is obtained with (1), therefore %IE lead to lower in the order: (1) > (2) > (3).

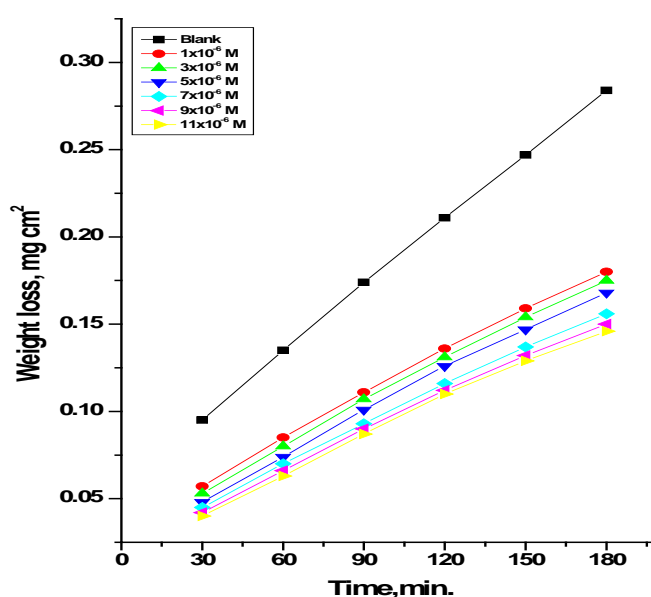


**Fig. 1.** Time-mass loss for C-steel liquefaction in 2 M hydrochloric acid attendance and lack of unlike dose of inhibitor (1).

**Table 2:** Variation of inhibition efficiency (%IE) of different quinolin-8-ol derivatives with their molar doses from mass reduction method at immersion 60 min in acidic solution.

Conc. (M)	(%IE)		
	(1)	(2)	(3)
			28.1
1x10 <sup>-6</sup>	37.0	32.6	
			32.6
3x10 <sup>-6</sup>	40.7	37.0	
			35.6
5x10 <sup>-6</sup>	45.2	40.7	
			37.8
7x10 <sup>-6</sup>	48.1	43.7	
			42.2
9x10 <sup>-6</sup>	51.1	45.9	
			45.19
11x10 <sup>-6</sup>	53.33	49.63	

### 3.1.1. Adsorption isotherm

The adsorption isotherm given best information onto the corrosion mechanism of inhibition as well as the reaction between the molecules adsorbed themselves and their reaction with the surface of electrode [28]. In this work, adsorption Freundlich isotherm was obtain to be best for the record results. The isotherm is given by the equation:

$$\log \theta = \log K + n \log C \tag{4}$$

$K_{ads}$  = equilibrium adsorption constant and  $C$  = dose of inhibitor. The draw of  $\log C$  against  $\log \theta$  was linear contact (Fig. 2). The  $K_{ads}$  can be measured from the intercept. Also  $\Delta G^{\circ}_{ads}$  can be measured from equation:

$$\log K_{ads} = - \log 55.5 - \Delta G^{\circ}_{ads} / 2.303 RT \tag{5}$$

$T$  = temperature absolute,  $R$  = constant universal gas and  $55.5$  = water dose in solution in M/L [29,30]. From Table 3, the values of  $K_{ads}$  were found to run parallel to the %IE [ $K$  of Compound (1) >  $K$

of Compound (2) > K of Compound (3)]. This data invert the rising capability, due to formation structural on surface of alloy [31].

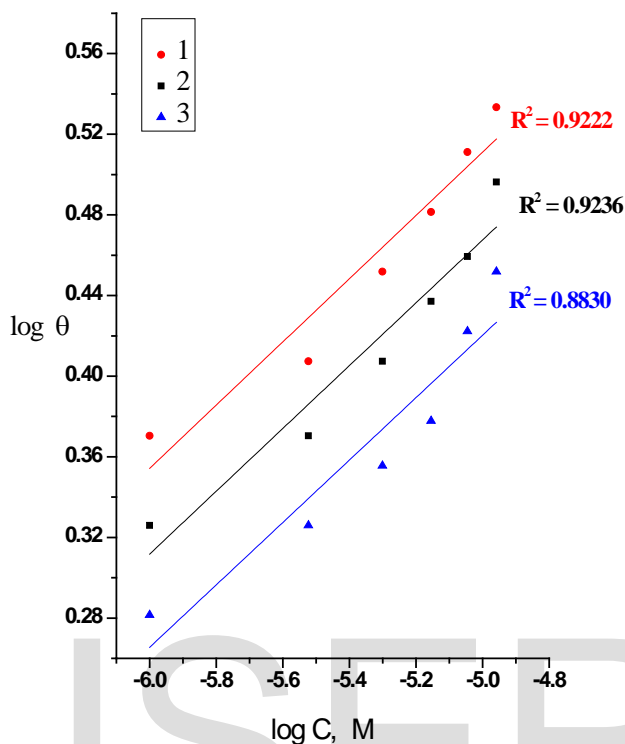


**Fig. 2.** Curve fitting of corrosion data for C-steel in 2 M HCl in presence of different concentrations of inhibitors to the Freundlich isotherm at  $30 \pm 0.1$  °C.

**Table 3:** Inhibitor binding constant ( $K_{ads}$ ) and free energy of binding ( $\Delta G_{ads}$ ) for inhibitors at  $30 \pm 0.1$  °C.

Inhibitor	Freundlich isotherm		
	n	$K_{ads}$ ( $M^{-1}$ )	$-\Delta G_{ads}$ ( $kJ\ mol^{-1}$ )
Compound (1)	14.876	1.348	10.872
Compound (2)	14.784	1.333	10.844
Compound (3)	14.684	1.322	10.822

### 3.1.2. Effect of temperature

The ( $E_a^*$ ) for the corrosion of alloy attendance and lack of unlike dose of quinolin-8-ol derivatives were measured utilized Arrhenius-kind equation [32]:

$$\log k = \log A - E_a^* / 2.303 RT \quad (6)$$

T = temperature absolute, k = constant rate, A = factor pre-exponential,  $E_a^*$  = activation energy apparent of the process corrosion and R = constant universal gas. Arrhenius curves of  $1/T$  vs.  $\log k$  for alloy in 2 M acid attendance and lack of unlike dose of inhibitor (1) are graphically given in Figure 3. The change of  $\log k$  against  $1/T$  is a line linear. The data of  $E_a^*$  were measured from the slope of these lines and record in Table 4. The rise  $E_a^*$  with inhibitors dose lead to rise energy barrier for corrosion reaction, the activation energy of the process corrosion is larger than  $20 \text{ kJ mol}^{-1}$  [33]. Enthalpy and entropy of activation ( $\Delta H^*$ ,  $\Delta S^*$ ) for the corrosion of alloy in 2 M HCl were given by performance the transition state (7):

$$k = (RT/Nh) \exp(\Delta S^*/R) \exp(-\Delta H^*/RT) \quad (7)$$

$N$  = Avogadro's number,  $h$  = constant Planck's. a curves  $\log k/T$  vs.  $1/T$  also gave lines straight as given in Fig. 4 for alloy liquefaction in 2 M acid attendance and lack of unlike dose of inhibitor (1). The intercept =  $\log RT/Nh + (\Delta S^*/2.303R)$  and lines slopes =  $-\Delta H^*/2.303R$  from which the data of  $\Delta H^*$  and  $\Delta S^*$  were record and tabulated in Table 4.

From these outcomes, the presences of compound improve the activation energy data and consequently lower the rate of corrosion of alloy. These data contain that these tested compounds play as inhibitors through rising activation energy of alloy liquefactions by given a barrier to mass and charge transfer by their adsorption on surface of alloy. Sign positive of the enthalpies invert the nature endothermic of the alloy liquefactions.

All  $E_a^*$  data are bigger than the analogous data of  $\Delta H^*$  lead to that the process of corrosion must contain a gaseous reaction, simply evolution of hydrogen, associated with a lower in the total volume reaction [34]. The data of  $\Delta S^*$  in lack and attendance of tested compounds are higher and negative; this led to that the activated complex in the rate-determining step prefer an association rather than dissociation step, i.e, lowering in disordering [35,36].

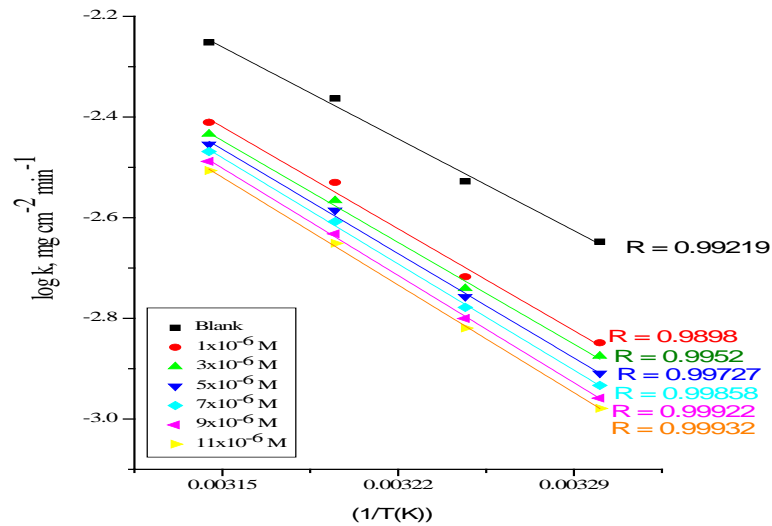


**Fig. 3.** Arrehenius plots ( $\log k$  vs.  $1/T$ ) for C-steel in 2 M hydrochloric acid attendance and lack of unlike dose of inhibitor (1)

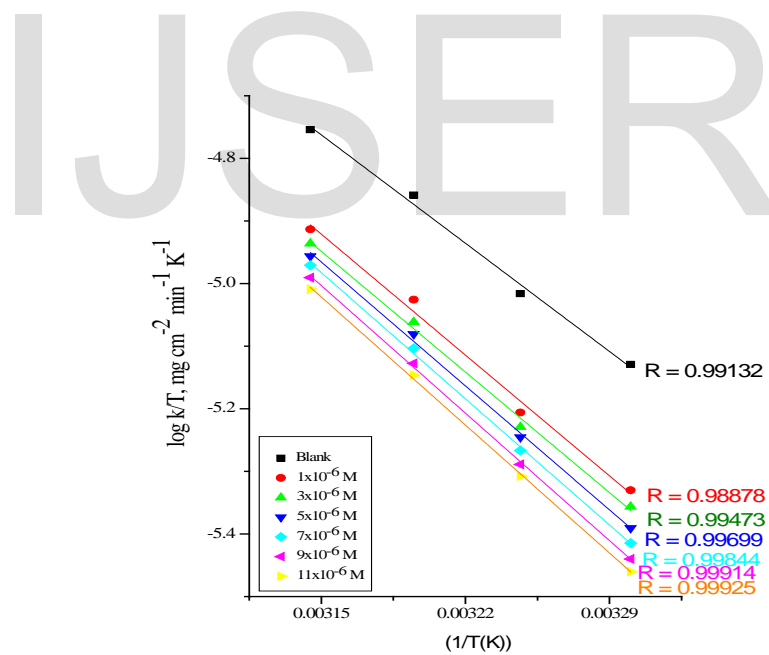


**Fig. 4.** Transition state plots ( $\log k/T$  vs.  $1/T$ ) for alloy in 2 M hydrochloric acid attendance and lack of unlike dose of inhibitor (1)



**Table 4.** Parameters of thermodynamic for the liquefaction of alloy in 2 M hydrochloric acid attendance and lack of unlike dose of ligands (HLn) from mass reduction tests at 60 min immersion.

Compound	Conc. (M)	$E_a^*$ (kJ mol <sup>-1</sup> )	$\Delta H^*$ (kJ mol <sup>-1</sup> )	$-\Delta S^*$ (J mol <sup>-1</sup> K <sup>-1</sup> )
Blank		49.90	47.30	139.62
(1)	1x10 <sup>-6</sup>	55.19	52.58	125.39
	3x10 <sup>-6</sup>	55.29	52.68	126.23
	5 x10 <sup>-6</sup>	56.73	54.12	127.02
	7x10 <sup>-6</sup>	57.71	55.10	129.26
	9x10 <sup>-6</sup>	58.30	55.69	130.80
	11x10 <sup>-6</sup>	58.51	55.90	131.48
(2)	1x10 <sup>-6</sup>	53.04	50.44	125.48
	3x10 <sup>-6</sup>	54.75	52.15	127.46
	5 x10 <sup>-6</sup>	56.17	53.56	129.29
	7x10 <sup>-6</sup>	55.59	52.98	129.58
	9x10 <sup>-6</sup>	56.85	54.24	131.82
	11x10 <sup>-6</sup>	58.12	55.01	132.48
(3)	1x10 <sup>-6</sup>	52.42	49.81	133.51
	3x10 <sup>-6</sup>	53.79	51.19	133.54
	5 x10 <sup>-6</sup>	55.72	52.11	134.92
	7x10 <sup>-6</sup>	55.38	52.77	135.57
	9x10 <sup>-6</sup>	56.22	53.61	136.81
	11x10 <sup>-6</sup>	57.32	54.71	137.63

### 3.2. Potentiodynamic polarization measurements

Polarization tests were done in order to gain knowledge concerning the kinetics of the cathodic and anodic reactions. Fig. 5 shows the polarization behavior of C-steel electrode in 2 M HCl without

and with unlike dose of inhibitor (1). Fig. 5 gives that both the cathodic and anodic reactions are impressive by the putting of investigated quinolin-8-ol derivatives and the protection efficiency improve as the inhibitor dose rise, but the cathodic reaction is more inhibited, i.e the addition of quinolin-8-ol derivatives lower the anodic liquefaction of alloy and also prevent the cathodic reactions. Therefore, quinolin-8-ol derivatives are play as mixed kind inhibitors.

The data in Table 5 given corrosion current density lower obviously after the appending of inhibitors in 2 M HCl and % IE rise with higher the dose of inhibitor. The  $E_{corr}$  with inhibitor was improve with no definite trend, lead to that these inhibitor play as mixed-kind inhibitors. %IE<sub>p</sub> was record by utilized equation:

$$\%IE_p = [(i_{corr}^0 - i_{corr}) / i_{corr}^0] \times 100 \quad (8)$$

where  $i_{corr}$  and  $i_{corr}^0$  are the inhibited and lack inhibited current corrosion densities, respectively.

It is evident from Table 5 that the ( $\beta_a$ ) and ( $\beta_c$ ) Tafel lines equal upon unchanged appending of organic derivatives, improvement to a nearly parallel set of anodic lines, and almost parallel cathodic curves record too. The inhibitors adsorbed lower the surface area for corrosion without impressive of the mechanism corrosion of alloy in acidic solution [37,38]. The orders of IE% were: (1) > (2) > (3). This order may lead to free electron pair in substituent in the molecular structure, N<sub>2</sub> atom and  $\pi$  electrons on aromatic nuclei of the inhibitor. This method confirmed from mass reduction tests, the rise in ability of (1) to inhibit in acidic corrosion of alloy as analogy to (3).

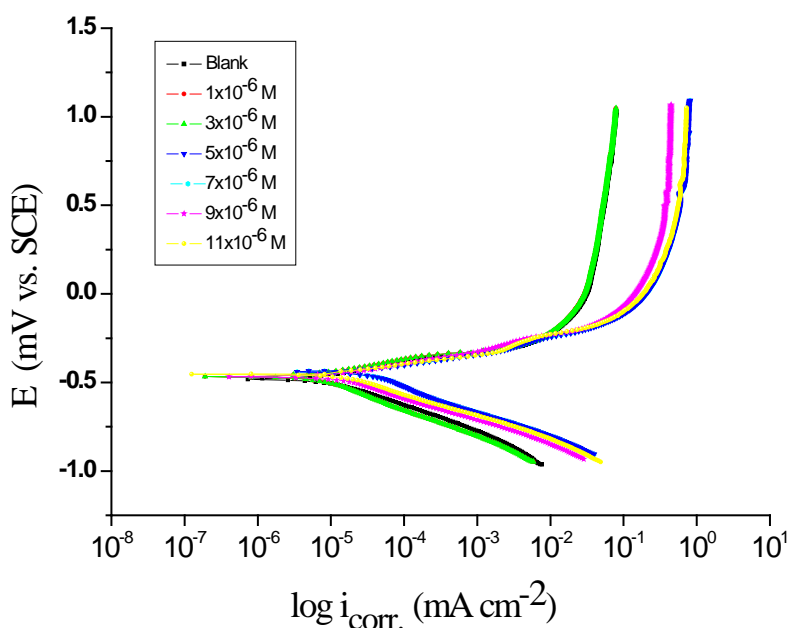


**Fig. 5.** Tafel polarization diagrams for the corrosion of alloy in 2 M HCl attendance and lack of unlike dose of inhibitor (1).

**Table 5:** Concentrations parameters effect of quinolin-8-ol derivatives for alloy in 2 M HCl attendances and lack of unlike dose of inhibitors.

Comp.	Conc., M.	$-E_{corr.}$ , mV(vs SCE)	$i_{corr.}$ $\mu\text{A cm}^{-2}$	$\beta_a$ , mV dec <sup>-1</sup>	$\beta_c$ , mV dec <sup>-1</sup>	$\theta$	% IE
(1)	Blank	494	6.00	81.1	126.8	----	-----
	$1 \times 10^{-6}$	472	1.80	40.6	66.2	0.700	70.0
	$3 \times 10^{-6}$	463	1.75	36.4	46.3	0.708	70.8
	$5 \times 10^{-6}$	486	1.75	65.1	96.2	0,713	71.3
	$7 \times 10^{-6}$	487	1.61	80.8	97.2	0.781	73.1
	$9 \times 10^{-6}$	491	1.57	81.7	106.0	0.738	73.8
	$11 \times 10^{-6}$	460	1.48	97.0	120.9	0.753	75.3
(2)	$1 \times 10^{-6}$	492	2.97	85.2	120.4	0.505	50.5
	$3 \times 10^{-6}$	472	2.79	78.8	101.6	0.535	53.5
	$5 \times 10^{-6}$	492	2.06	85.2	120.4	0.656	65.6
	$7 \times 10^{-6}$	472	2.01	78.9	101.6	0.665	66.5
	$9 \times 10^{-6}$	448	1.87	70.4	114.5	0.688	68.8
	$11 \times 10^{-6}$	483	1.82	69.0	107.1	0.696	69.6
(3)	$1 \times 10^{-6}$	481	4.80	78.4	123.7	0.20	20.0
	$3 \times 10^{-6}$	489	4.48	77.9	109.1	0.253	25.3
	$5 \times 10^{-6}$	467	4.04	81.4	118.1	0.326	32.6
	$7 \times 10^{-6}$	459	3.55	77.6	106.1	0.408	40.8
	$9 \times 10^{-6}$	497	3.073	82.1	111.2	0.487	48.7
	$11 \times 10^{-6}$	477	3.04	95.3	114.7	0.493	49.3

### 3.3. (EIS) tests

EIS is a powerful method in the research of corrosion. Mechanistic information, properties of surface and kinetics of electrode can be given from impedance plots [39-40]. Figure 6 given Nyquist (a) and Bode (b) curves given at open-circuit potential both in lack and attendance of rising dose of investigated quinolin-8-ol derivatives. The improvement in the size of the capacitive loop with the appending of quinolin-8-ol derivatives gives that a gradually barrier forms on the alloy surface. The rise in the size of capacitive loop Fig. 6(a) enhances, at a fixed inhibitor dose, obeyed the order: (1) > (2) > (3).

The Nyquist digrames do not given best semicircles as theory expected of EIS. The change from ideal semicircle due to the dispersion of frequency [41] as well as to the inhomogeneity's of the surface. EIS of the additives organic were calculated utilized the equivalent circuit, Fig. 7, the best fit circuit in our experimental data results [42]. The  $C_{dl}$  (double layer capacitance) is measured from Eq. (9):

$$C_{dl} = Y_o \omega^{n-1} / \sin [n (\pi/2)] \quad (9)$$

where  $Y_o$  = CPE magnitude,  $\omega = 2\pi f_{max}$ ,  $f_{max}$  = the imaginary frequency at which the component of the impedance is maximal.

After test the shape of the Nyquist curves, the corrosion process was controlled mainly charged-transfer [43-44]. From the EIS data (Table 6), we noted that the data of  $R_{ct}$  rise with rising the dose of the inhibitors and this lead to an rise in % IE, which in obeys with the mass reduction results given. Data of capacitance double layer are also lower to the maximum inhibitor extent. The lower in CPE/ $C_{dl}$  data from a lower in local dielectric constant and/or an improve in the double layer thickness, given that organic derivatives protect the alloy from corrosion [45]. The main advantages of EIS are to follow the corrosion behavior of the metal with constant time. The inhibition efficiency was calculated from the charge transfer resistance data from equation (10) [46]:

$$\% IE_{EIS} = [1 - (R_{ct}^o / R_{ct})] \times 100 \quad (10)$$

where  $R_{ct}^o$  and  $R_{ct}$  are the charge-transfer resistance values without and with inhibitor, consecutively.

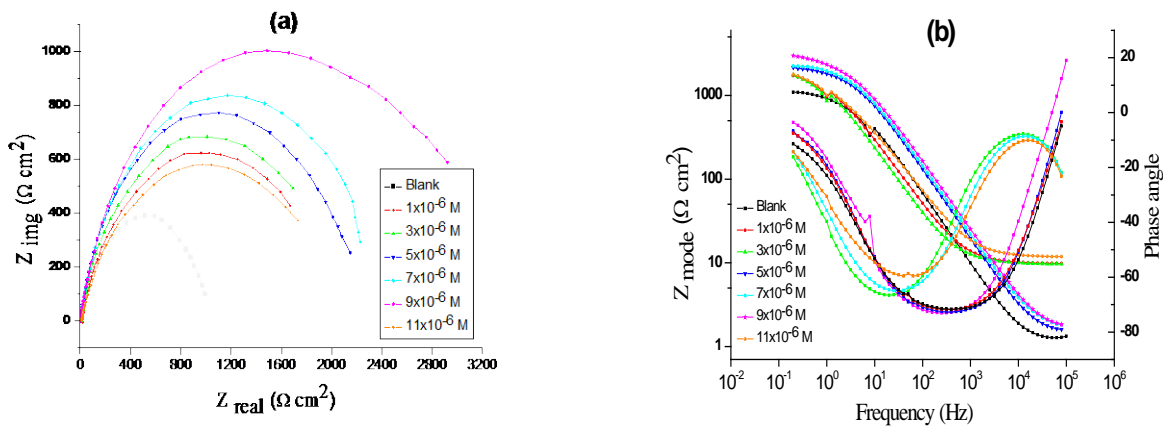


**Fig. 6.** EIS Nyquist (a) and Bode diagrams (b) for the corrosion of alloy in 2 M hydrochloric acid attendance and lack of unlike dose of inhibitor(1).

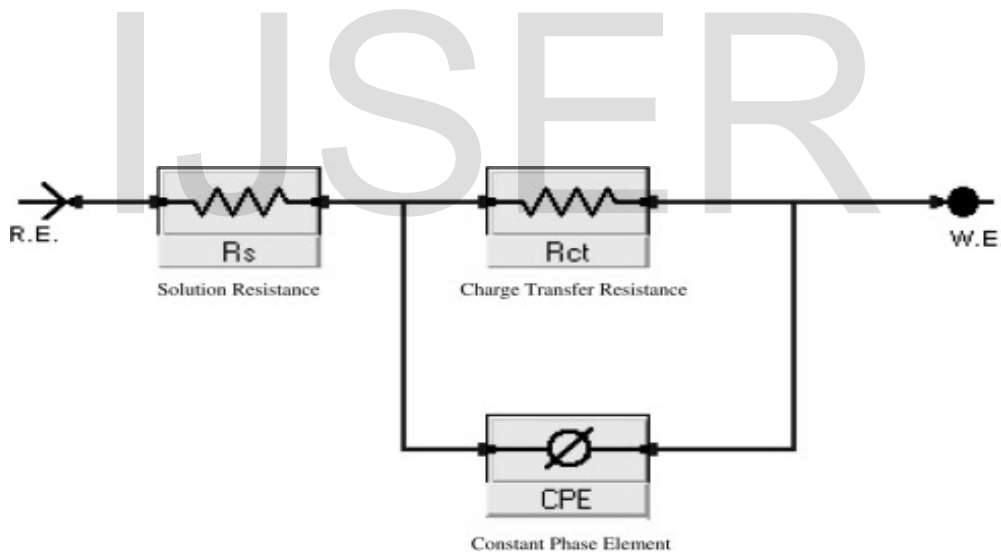


**Fig. 7.** Circuit equivalent utilized to fit EIS data.

**Table 6:** kinetic parameters given by EIS test for alloy in 2 M HCl attendance and lack of unlike dose of quinolin-8-ol derivatives at  $30 \pm 0.1$  °C.

Comp.	Conc., M .	$R_s, \Omega \text{cm}^2$	$Y_o, \times 10^{-3} \mu\Omega^{-1} s^n$	n	$R_{ct}, \Omega \text{cm}^2$	$C_{dl}, \mu\text{Fcm}^{-2}$	$\theta$	IE

(1)	Blank	1.570	352.1	878.2	40.40	69.68	-----	
	$1 \times 10^{-6}$	1.275	341.8	887.5	51.36	19.689	0.7178	71.78
	$3 \times 10^{-6}$	1.566	219.5	898.9	50.08	17.39	0.7505	75.05
	$5 \times 10^{-6}$	1.500	303.1	897.5	60.33	16.75	0.7598	75.98
	$7 \times 10^{-6}$	1.817	398.1	851.7	60.96	16.59	0.7623	76.23
	$9 \times 10^{-6}$	2.211	260.4	885.5	85.73	11.74	0.8309	83.09
	$11 \times 10^{-6}$	2.452	112.0	868.3	267.6	37.81	0.9458	94.58
(2)	$1 \times 10^{-6}$	1.344	389.8	880.5	28.48	35.48	0.4912	49.12
	$3 \times 10^{-6}$	1.519	357.0	889.6	28.91	34.95	0.4987	49.87
	$5 \times 10^{-6}$	1.499	246.3	901.1	32.42	3.117	0.5527	55.27
	$7 \times 10^{-6}$	1.474	279.3	900.6	40.87	24.72	0.6454	64.54
	$9 \times 10^{-6}$	1.776	400.0	866.7	42.2	23.96	0.6566	65.66
	$11 \times 10^{-6}$	1.543	208.0	888.0	50.45	20.029	0.7127	71.27
(3)	$1 \times 10^{-6}$	1.54	284.2	892.5	17.97	56.18	0.1936	19.36
	$3 \times 10^{-6}$	1.38	262.0	895.0	19.29	52.336	0.2488	24.88
	$5 \times 10^{-6}$	1.346	266.5	878.0	19.72	51.207	0.2652	26.52
	$7 \times 10^{-6}$	1.830	301.9	872.1	20.91	48.306	0.3070	30.70
	$9 \times 10^{-6}$	1.458	303.1	866.3	23.34	43.28	0.3791	37.91
	$11 \times 10^{-6}$	1.791	211.0	875.7	28.42	35.91	0.4847	48.47

### 3.4. EFM method

The advantages of EFM test give it an ideal for online monitoring of corrosion [47]. The causality factors is higher strength data of the EFM which act as an internal check on verified data and of the EFM test. The CF-2 and CF-3 are record from the frequency spectrum of the responses current.

The data of (EFM) in acidic solution with and without various doses of quinolin-8-ol derivatives given in Fig. 8. The same plots were obtained for other compounds (not shown). The two higher peaks, with amplitude of about 200  $\mu\text{A}$ , are the given to the 40 and 100 mHz (2 and 5 Hz) excitation frequencies. The EFM experimental data were utilized two unlike models: diffusion complete control of the cathodic reaction and the “activation” model [48]. The higher peaks were utilized to measure the ( $i_{\text{corr}}$ ), (CF-2 and CF-3) and ( $\beta_c$  and  $\beta_a$ ). The EFM parameters were given in Table 7 show that, the appended of any one of tested compounds at a given dose to the acidic solution lower the current corrosion density, lead to these compounds protect the corrosion of alloy through adsorption. The best data of CF-2 and CF-3 in Table (7) are similar to their theoretical data of 2.0 and 3.0, respectively lead to the calculated value are quality good.

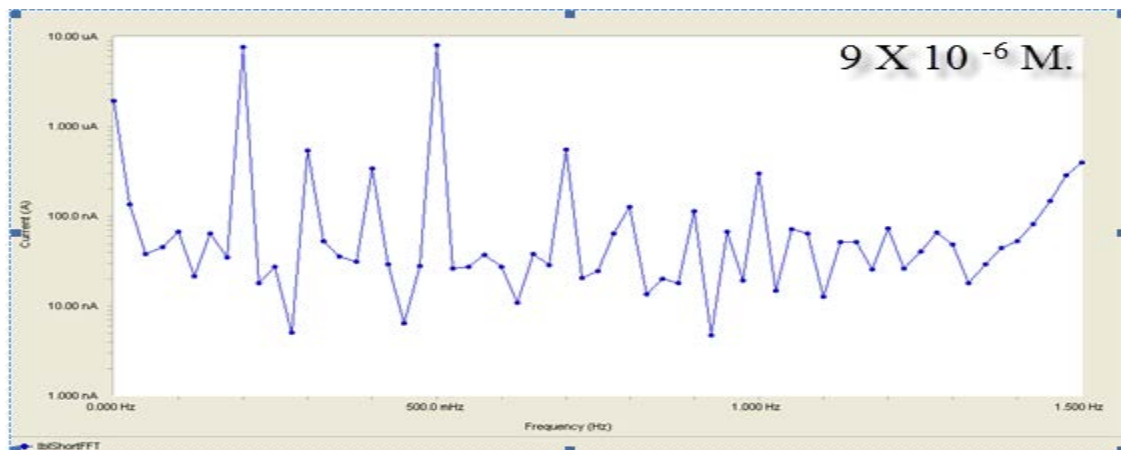
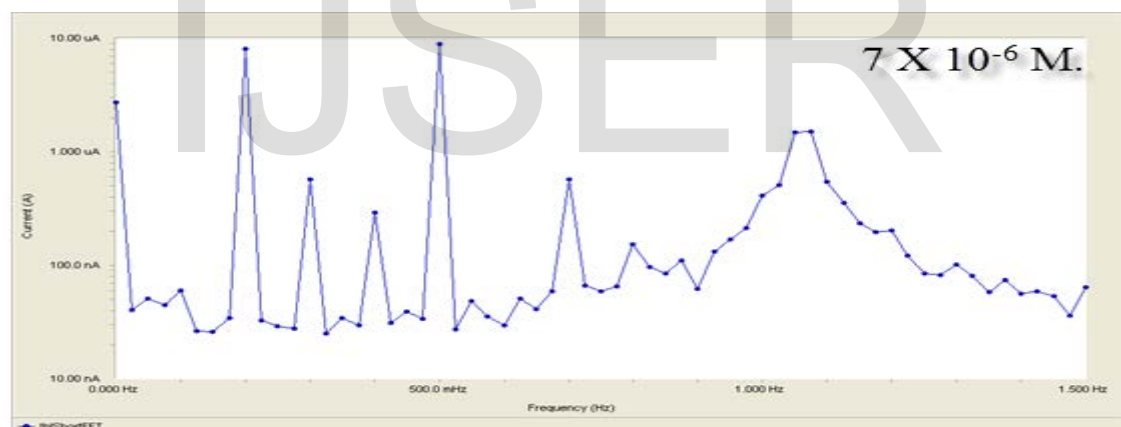
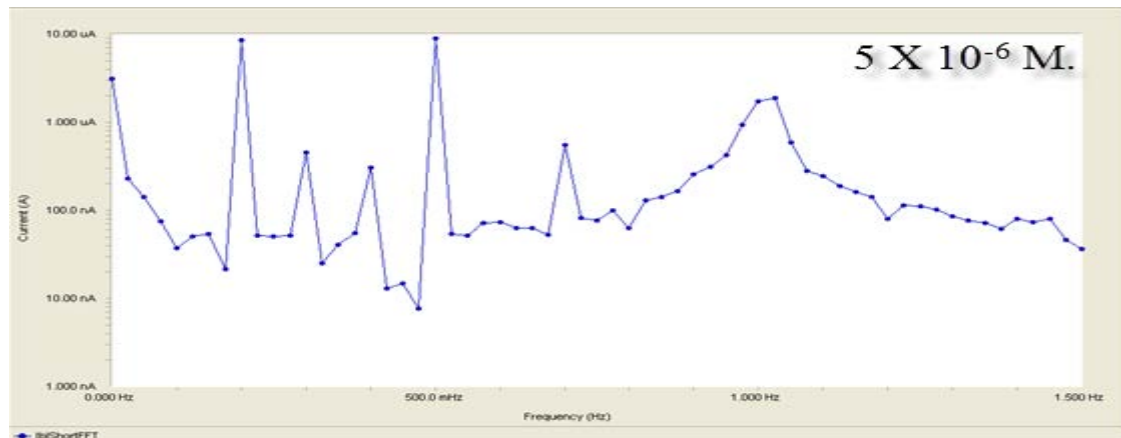
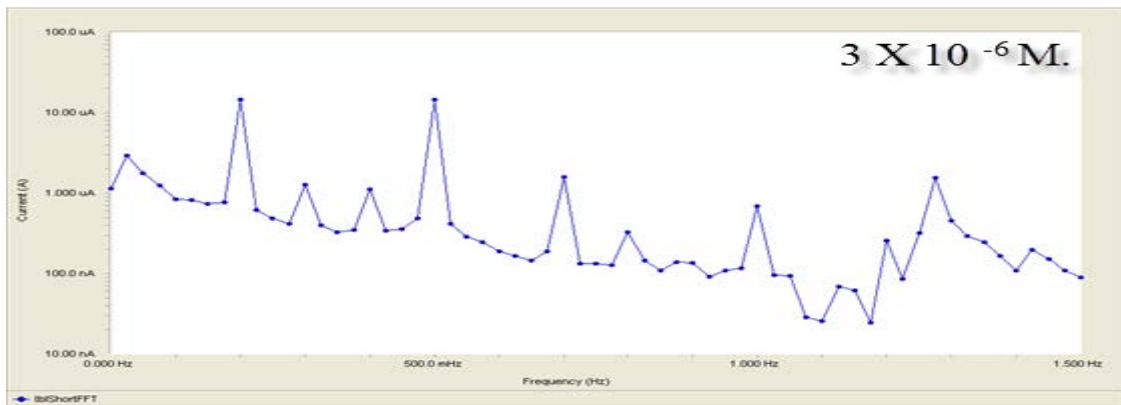
The %  $\text{IE}_{\text{EFM}}$  improves by raising the inhibitor dose and was measured from equation (11):

$$\% \text{IE}_{\text{EFM}} = [1 - (i_{\text{corr}} / i_{\text{corr}}^0)] \times 100 \quad (11)$$

where  $i_{\text{corr}}^0$  and  $i_{\text{corr}}$  are current corrosion densities without and with inhibitor, consecutively.

The order of %  $\text{IE}_{\text{EFM}}$  : (1) > (2) > (3).







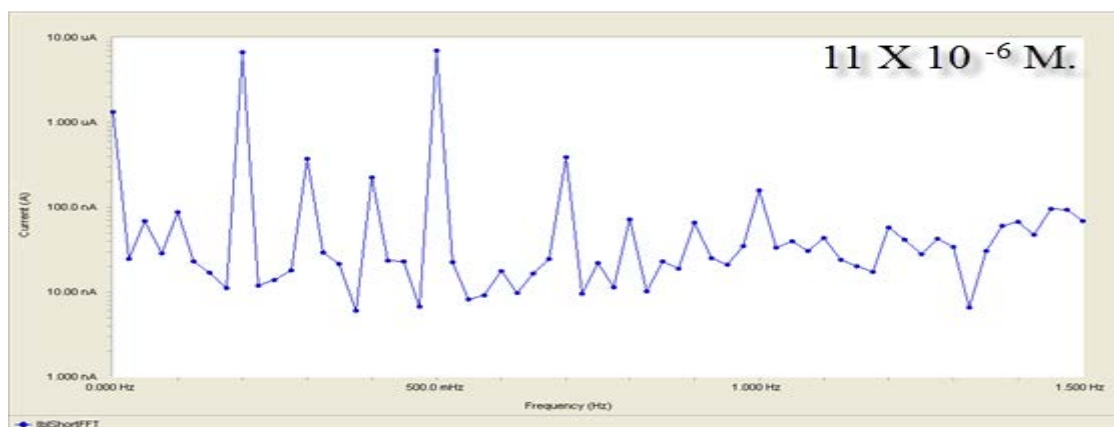


**Fig. 8.** EFM spectra for the corrosion of alloy in 2 M HCl attendance and lack of unlike dose of inhibitor (1).

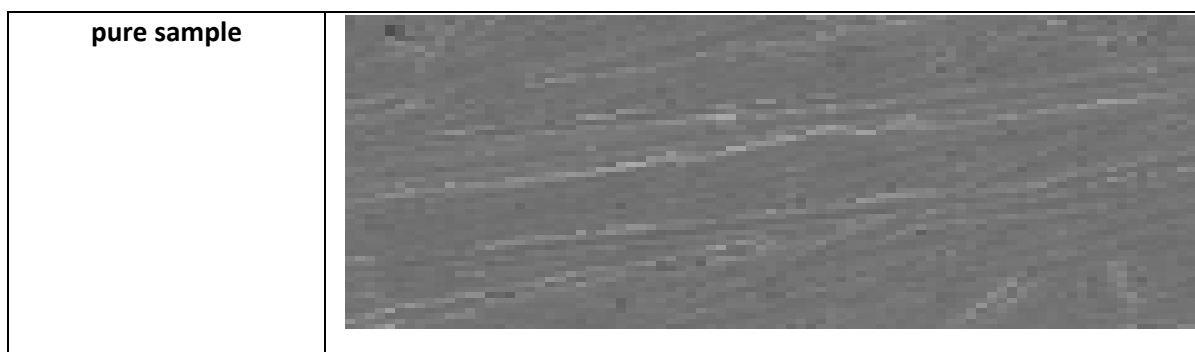
**Table 7:** Electrochemical kinetic parameters obtained by EFM technique for C-steel in 2 M HCl without and with various concentrations of quinolin-8-ol derivatives at  $30 \pm 0.1$  °C.

Comp.	Conc.,M .	$I_{corr} \mu Acm^{-2}$	$\beta_c$ $mVdec^{-1}$	$\beta_a$ $mVdec^{-1}$	CF-2	CF-3	$\theta$	%IE
	Blank	909.3	121.8	161.1	1.97	3.09	-	-
(1)	$1 \times 10^{-6}$	231.8	38.5	39.2	2.06	2.97	0.745	74.5
	$3 \times 10^{-6}$	179.0	51.5	53.3	1.89	2.93	0.803	80.3
	$5 \times 10^{-6}$	175.3	48.5	51.6	1.88	2.89	0.807	80.7
	$7 \times 10^{-6}$	170.3	45.7	48.4	2.03	3.09	0.812	81.2
	$9 \times 10^{-6}$	115.2	43.6	50.7	2.01	3.07	0.873	87.3
	$11 \times 10^{-6}$	50.49	74.1	77.2	1.95	2.99	0.944	94.4
(2)	$1 \times 10^{-6}$	294.0	78.8	89.9	2.04	2.89	0.676	67.6
	$3 \times 10^{-6}$	291.7	33.1	33.8	1.86	3.02	0.679	67.9
	$5 \times 10^{-6}$	283.3	26.9	28.1	1.92	3.07	0.688	68.8

	$7 \times 10^{-6}$	282.2	32.9	33.7	2.02	3.01	0.689	68.9
	$9 \times 10^{-6}$	273.3	30.9	32.6	2.01	2.89	0.699	69.9
	$11 \times 10^{-6}$	248.6	54.5	60.4	1.89	2.95	0.726	72.6
(3)	$1 \times 10^{-6}$	548.9	97.4	115.4	1.93	2.27	0.397	39.73
	$3 \times 10^{-6}$	537.6	94.4	114.2	1.88	2.85	0.408	40.8
	$5 \times 10^{-6}$	444.9	65.4	70.11	2.06	3.03	0.511	51.07
	$7 \times 10^{-6}$	401.1	85.3	107.4	1.93	2.92	0.558	55.8
	$9 \times 10^{-6}$	400.4	84.4	56.8	1.95	2.93	0.559	55.9
	$11 \times 10^{-6}$	359.5	41.8	43.3	1.89	3.01	0.604	60.4

### 3.5. (SEM) tests

The micrograph given from coins of alloy without and with of  $11 \times 10^{-6}$  M quinolin-8-ol derivatives after putted for 3 days given in Fig. 9. The surfaces suffer from severe corrosion attack in the blank sample. Due to the stress out when the compound adding in the solution, the morphology of alloy surfaces is quite unlike from the preceding one, and the tests surfaces were smoother. We observed a film formation which distributed in a random way on the whole alloy surface. This may be interpreted as due to the adsorption of the quinolin-8-ol derivatives on alloy surface merger into the passive film in order to the active site block on alloy. Resulting in a lower in the contact among alloy and the aggressive medium and sequentially obtain best inhibition effect [49].



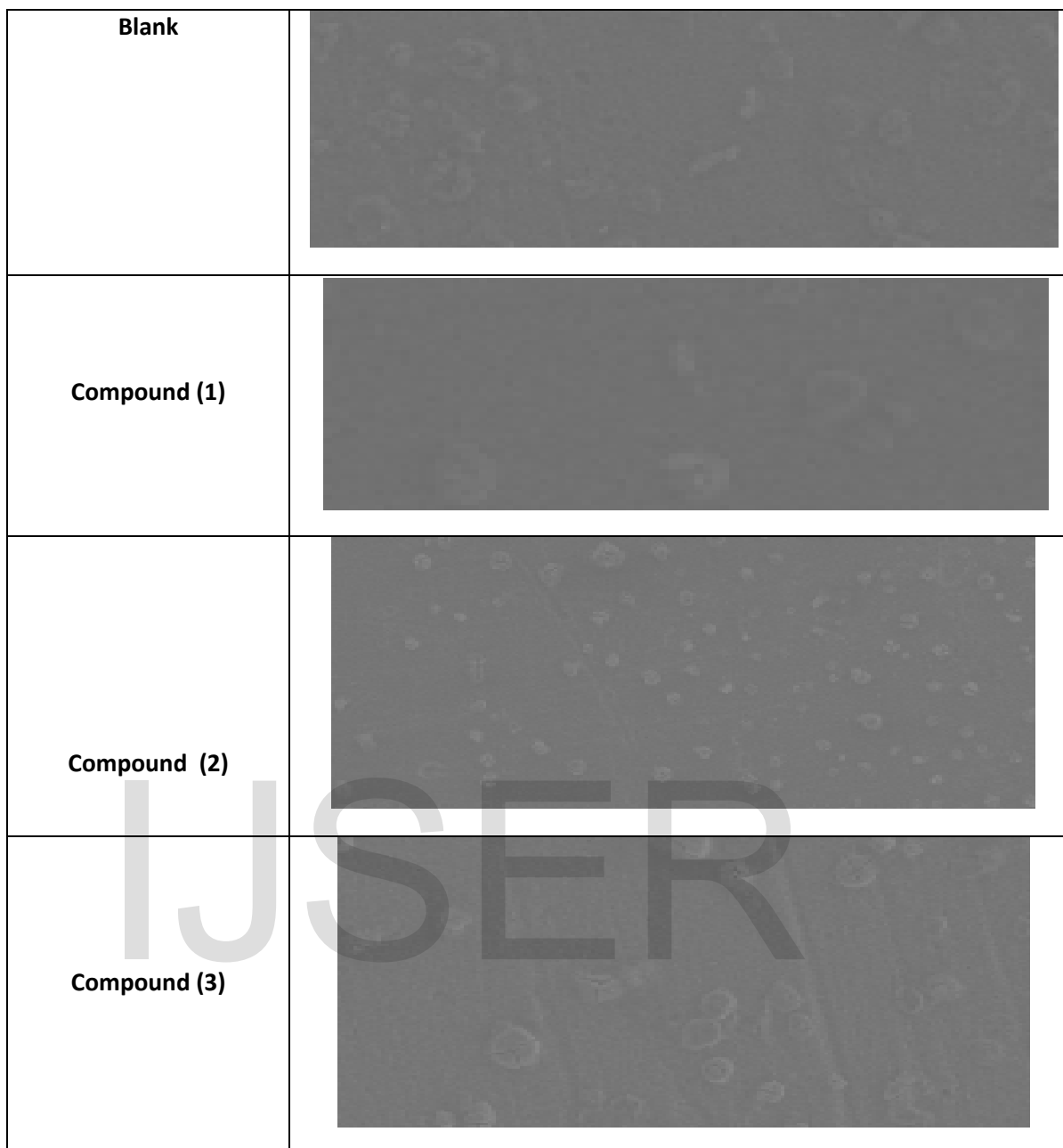


**Fig. 9.** SEM images of C-steel in 2 M HCl solution after immersion for 3 hrs without inhibitor and with of  $11 \times 10^{-6}$  M of quinolin-8-ol derivatives .

### 3.6. (EDS) test

The EDS spectra were utilized to measure the elements found on the surface of alloy and after 3 days of covered in the lack and attendance of 2M HCl. Fig. 10 gives the EDS result measured on the composition of alloy only without the acid and inhibitor modified. The EDS record that only oxygen and iron were observed, which given that the passive film found with only  $Fe_2O_3$ .

The EDS tests of alloy in 2 M HCl only and with of  $11 \times 10^{-6}$  M of quinolin-8-ol derivatives portrays in Fig. 10. The spectra give additional lines, lead to the presence of C (the carbon atoms of

quinolin-8-ol derivatives). These values gives that the O and C atoms covered surface. The elemental observed is record in Table 8.

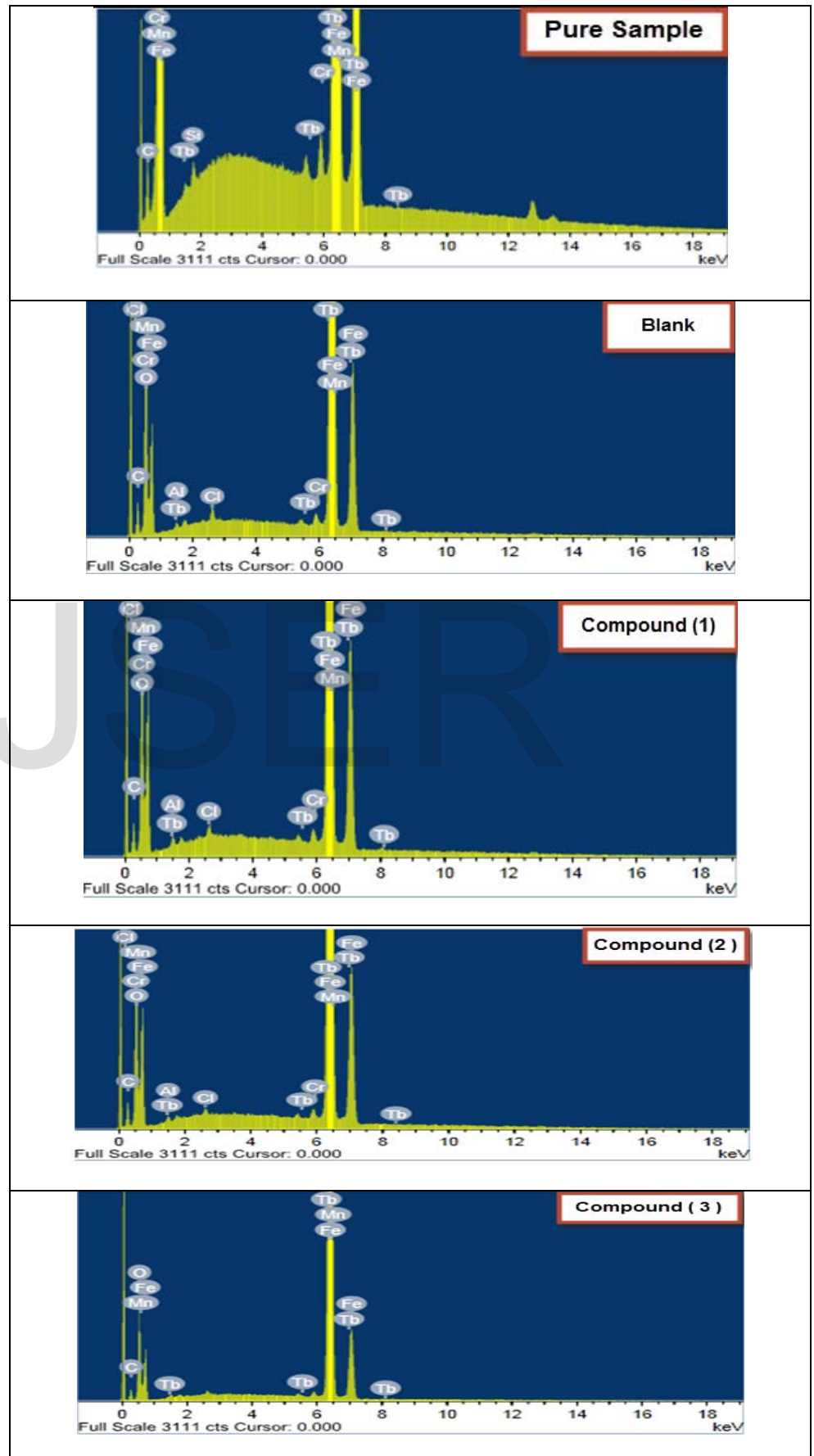


**Fig. 10.** EDS study of C-steel in 2 M HCl solution after immersion for 3 hrs without inhibitor and in presence of  $11 \times 10^{-6}$  M of quinolin-8-ol derivatives .

**Table 8:** Wt % of C-steel after 3 days in 2 M HCl lack and attendance of the optimum dose of the studied quinolin-8-ol derivatives.

(Mass %)	C	O	Al	Si	Cr	Mn	Fe	Tb	Cl
Pure Sample	6.78	----	0.29	0.28	0.22	0.47	87.53	4.43	----
Blank	10.99	21.58	0.30	----	0.16	0.34	62.75	---	0.33
Compound (1)	8.99	19.45	0.40	----	0.17	0.40	66.78	3.58	----
Compound (2)	9.70	19.10	0.33	----	0.18	0.36	66.51	3.61	----
Compound (3)	9.51	21.01	----	----	---	0.45	66.10	2.93	----

### 3.7. Mechanism of Corrosion protection

From the chemical and electrochemical experiments the IE% relies on dose, metal nature, surface conditions and the type of inhibitors adsorption on alloy.

The results of corrosion value attendance of these inhibitors:

- i) The lower of rate and current of corrosion with rise in dose of the inhibitor.
- ii) The linear different of mass reduction with time.
- iii) The change in Tafel lines to maximum regions of potential.
- iv) The lower in IE% corrosion with improve temperature lead to desorption of the adsorbed inhibitor molecules obtain.
- v) The %IE relies on charge density and their equipment of adsorption centers in the molecule.

It was observed that the type of adsorption relies on the affinity of the alloy towards the clouds of  $\pi$ -electron of the ring. Metals such as iron, which have a higher attract towards aromatic moieties, were obtain to adsorb benzene rings in orientation flat. The order of lowering the % IE are given: 1 > 2 > 3.

5-(2-(4-Methoxyphenyl)diazenyl)quinolin-8-ol (Compound (1)) found best power inhibition due to: (i) the presence of  $p$ -OCH<sub>3</sub> group which is an electron donating group with negative Hammett constant ( $\sigma = -0.27$ ), Also this group will rise the electron density charge on the molecule, and (ii) its biggest size of molecular that may easy better surface hedge. Inhibitor (2) found after (1) in IE%. This

is due to it has lesser size and has no replacement in *p*-position. The lower % IE Inhibitor (3) due to the attendance of *p*-Cl which has positive Hammett constant ( $\sigma_{Cl} = + 0.23$ )

## Conclusion

- 1- All the investigated compounds are good corrosion inhibitors for C- steel in 2 M HCl solution. The effectiveness of these inhibitors depends on their structures. The variation in inhibitive efficiency depends on the type and the nature of the substituent present in the inhibitor molecule.
- 2- The inhibitors are adsorbed on C- steel surface follows the Freundlich model isotherm
- 3- Double layer capacitances decrease with respect to blank solution when the inhibitor added. This fact may explained by adsorption of the inhibitor molecule on the C-steel surface.
- 4- EFM can be utilized as a fast and nondestructive tests for calculation of corrosion without prior information of Tafel lines
- 5- The data from electrochemical and chemical tests were in best agreement. The % IE of these compounds investigated is:  $1 > 2 > 3$ .
- 6- The heteroatoms N and O are the active sites of the quinolin-8-ol derivatives. It can adsorb on Fe surface firmly by donating electrons to Fe atoms and accepting electrons from 3d orbital of Fe atoms.

## References

1. M.H. Wahdan, A.A. Hermas, M.S. Morad, Mater. Chem. Phys. 76 (2002) 111-118.
2. F. Bentiss, M. Lebrini, H. Vezin, M. Lagrenee, Mater. Chem. Phys. 87 (2004) 18-23.
3. X. Liu, P.C. Okafor, Y.G. Zheng, Corros. Sci. 51 (2009) 744-751.
4. A. Al Maofari, G. Ezznaydy, Y. Idouli, F. Guedira, S. Zaydoun, N. Labjar and S. El Hajjaji, J. Mater. Environ. Sci. 5 (2014) 2081- 2085.
5. K. Barouni, A. Kassale, A. Albourine, O. Jbara, B. Hammouti, L. Bazzi, J. Mater. Environ. Sci. 5 (2014) 456-463.
6. A.S. Fouda, K. Shalabi, H. Elmogazy, J. Mater. Environ. Sci. 5 (2014) 1691-1702.
7. A. Ostovari, S.M. Hoseinie, M. Peikari, S.R. Shadizadeh, S.J. Hashemi, Corros. Sci. 51 (2009) 1935-1949.
8. M.J. Bahrami, S.M.A. Hosseinia, P. Pilvar, Corros. Sci. 52 (2010) 2793-2803.
9. M.M. Solomon, S.A. Umoren, I.I. Udosoro, A.P. Udoh, Corros. Sci. 52 (2010) 1317-1325.
10. H.L. Wang, R.B. Liu, J. Xin, Corros. Sci. 46 (2004) 2455-2466.
11. R. Solmaz, G. Kardas, B. Yazici, M. Erbil, Prot. Met. 41 (2005) 581-585.
12. K.C. Emregul, R. Kurtaran, O. Atakol, Corros. Sci. 45 (2003) 2803-2817.
13. D. Chebabe, Z.A. Chikh, N. Hajjaji, A. Srhiri, F. Zucchi, Corros. Sci. 45 (2003) 309-320.

14. F.G. Liu, M. Du, J. Zhang, M. Qiu, *Corros. Sci.* 51 (2009) 102-109.
15. A.Y. Musa, A.A.H. Kadhum, A.B. Mohamad, M.S. Takriff, *Corros. Sci.* 52 (2010) 3331-3340.
16. K.F. Khaled, M.A. Amin, *Corros. Sci.* 51 (2009) 1964-1975.
17. M.A. Quraishi, M.Z.A. Rafiquee, S. Khan, N. Saxena, *J. Appl. Electrochem.* 37 (2007) 1153-1162.
18. X.Y. Zhang, F.P. Wang, Y.F. He, Y. Du, *Corros. Sci.* 43 (2001)1417-1431.
19. M. Knag, K. Bilkova, E. Gulbrandsen, P. Carlsen, J. Sjöblöm, *Corros. Sci.* 48 (2006) 2592-2613.
20. L. Wang, G.J. Yin, J.G. Yin, *Corros. Sci.* 43 (2001) 1197-1202.
21. P.C. Okafor, X. Liu, Y.G. Zheng, *Corros. Sci.* 51 (2009) 761-768.
22. J. Zhang, J.X. Liu, W.Z. Yu, Y.G. Yan, L. You, L.F. Liu, *Corros. Sci.* 52 (2010) 2059-2065.
23. A.M. Eldesoky, M.A. El-Bindary, A.Z. El-Sonbati, Sh.M. Morgan, *J. Mater. Environ. Sci.* 6 (2015) 2260-2276.
24. A.M. Eldesoky, M.A. Diab, A.A. El-Bindary, A.Z. El-Sonbati, H.A. Seyam, *J. Mater. Environ. Sci.* 6 (2015) 2148-2165.
25. A.Z. El-Sonbati, M.A. Diab, A.A. El-Bindary, A.F. Shoair, N.M. Beshry, *J. Mol. Liq.* 218 (2016) 400-420.
26. N.A. El-Ghamaz, A.A. El-Bindary, A.Z. El-Sonbati, N.M. Beshry, *J. Mol. Liq.* 211 (2015) 628-639
27. A.F. Shoair, A.A. El-Bindary, A.Z. El-Sonbati, N.M. Beshry, *J. Mol. Liq.* 215 (2016) 740-748.
28. A.N. Wiercinska, G. Dalmata, *Electrochim. Acta* 51 (2006) 6179-6185.
29. A. Yurt, A. Balaban, S.U. Kandemir, G. Bereket, B. Erk, *Mater. Chem. Phys.* 85 (2004) 420- 426.
30. A.Y. Etre, *Appl. Surf. Sci.* 252 (2006) 8521-8525.
31. W.J. Lorenz, F. Mansfeld, *Corros. Sci.* 21 (1981) 647-672.
32. I.N. Putilova, S.A. Balezin, V.P. Barannik, "Metallic Corrosion Inhibitors Pergamon" Press NewYork, 1960.
33. K.K. Al-Neami, A.K. Mohamed, I.M. Kenawy, A.S. Fouda, *Monatsh. Chem.* 126 (1995) 369- 376.
34. E.A. Noor, *Int. J. Electrochem. Sci.* 2(2007) 996-1017.
35. J. Marsh, *Advanced Organic Chemistry 3rd ed Wiley Eastern New Delhi* (1988).
36. S. Martinez, I. Stern, *Appl.Surf.Sci.* 199 (2002) 83-89.
37. M.A. Al-Khalidi, K.Y. Al-qahtani, *J. Mater. Environ. Sci.* 4 (5) (2013) 593-600.
38. J.W. Schlitze, K. Wippermann, *Electrochim. Acta* 32 (1987) 823-831.
39. D.C. Silverman, J.E. Carrico, *Corrosion* 44 (1988) 280- 287.

40. M. El Achouri, S. Kertit, H.M. Gouttaya, B. Nciri, Y. Bensouda, L. Perez, M.R. Infante, K. Elkacemi, *Prog. Org. Coat.* 43 (2001) 267-273.
41. A. Anejjar, A. Zarrouk, R. Salghi, H. Zarrok, D. Ben Hmamou, B. Hammouti, B. Elmahi, S.S. Al-Deyab, *J. Mater. Environ. Sci.* 4 (2013) 583-592.
42. S.F. Mertens, C. Xhoffer, B.C. Decooman, E. Temmerman, *Corrosion* 53 (1997) 381-388.
43. G. Trabanelli, C. Montecelli, V. Grassi, A. Frignani, *J. Cem. Concr. Res.* 35 (2005) 1804-1813.
44. M. Lagrenée, B. Mernari, M. Bouanis, M. Traisnel, F. Bentiss, *Corros. Sci.* 44 (2002) 573-588.
45. H. Ma, S. Chen, L. Niu, S. Zhao, S. Li, D. Li, *J. Appl. Electrochem.* 32 (2002) 65-72.
46. E. Kuş, F. Mansfeld, *Corros. Sci.* 48 (2006) 965-979.
47. G.A. Caignan, S.K. Metcalf, E.M. Holt, *J. Chem. Cryst.* 30 (2000) 415-422.
48. F. Samie, J. Tidblad, V. Kucera, C. Leygraf, *Atmospheric Environ.* 39 (2005) 7362-7373.
49. R.A. Prabhu, T.V. Venkatesha, A.V. Shanbhag, G.M. Kulkarni, R.G. Kalkhambkar, *Corros. Sci.* 50 (2008) 3356.

IJSER